Biointerface Research in Applied Chemistry
Open-Access Journal (ISSN: 2069-5837)

Research Article
Volume 14, Issue 1, 2024, 22
https://doi.org/10.33263/BRIAC141.022

Evaluation and Screening of *Hygrophila Schulli* Mediated Novel Antiproliferative Agent Against Lung Cancer Cell Line (A549) by *in vitro*

Sangilimuthu Alagar Yadav [1,*], Reshma Padikkayil [1], SowmyaPriya Manoharan [1], Ravi Subban [2], Kokou Atchou [3]

[1] Department of Biotechnology, Karpagam Academy of Higher Education, Coimbatore – 641 021, Tamil Nadu, India
[2] Department of Chemistry, Karpagam Academy of Higher Education, Coimbatore – 641 021, Tamil Nadu, India
[3] Laboratory of Physiology-Pharmacology, Unit of Pathophysiology, Bioactive Substances and Safety, Faculty of Sciences, University of Lome, Togo
* Correspondence: smuthu.al@gmail.com;

Scopus Author ID 55353524800
Received: 7.01.2023; Accepted: 22.02.2023; Published: 3.02.2024

Abstract: Lung cancer is the major type of cancer and produces a high prevalence rate worldwide. The scientific communities have attempted to find natural remedies for cancer treatment because synthetic medicines produce numerous side effects. Medicinal plants used in the Ayurvedic system and other natural medicines are increasingly studied for their effectiveness and lower side effects. This study aimed to isolate the leaves of Hygrophila Schulli from the molecule and evaluate their antioxidant and antiproliferative effects. Total phenolic, flavonoid, and alkaloid contents were determined in organic solvent extracts of *H. schulli* leaves. Antioxidant and antiproliferative effects against synthetic free radicals and human lung cancer cell line (A549) were determined using suitable *In vitro* methods, respectively. Effective extracts of *H. Schulli* were used to isolate the active molecule by column chromatography, followed by UV-Vis, FT-IR, NMR, and GC-MS spectral studies were performed in order to predict the structural elucidation of isolated compounds. Molecular docking was employed to examine the binding efficacy of the phytoconstituents on the Epidermal Growth Factor Receptor (EGFR). The methanolic and chloroform extracts exhibited diverse phytochemicals with considerable antioxidant and antiproliferative effects. A novel pentaene type molecule as (5E,9Z,13Z)-2, 6, 10, 14, 18-pentamethylnonadeca-1, 5, 9, 13, 17-pentaene from chloroform extract showed good antioxidant and antiproliferative effects as well as high binding properties with EGFR. Also, the pentaene compound induced cell cycle arrest in A549 cell lines at the G2/M phase by Flow cytometric analysis. Chloroform extract exerted evident antiproliferative effects attributed to the presence of a novel pentane compound. These findings provide a lead molecule from *H. schulli* leaves, a candidate drug for the invention of anticancer drugs.

Keywords: *Hygrophila schulli*; phytochemical structure; antioxidant; anticancer agent; human A549 lung cancer; EGFR binding.

1. Introduction

The almost evolution of all human diseases or disorders is mainly incorporated with oxidative stress due to the synthesis of free radicals. Free radicals are fundamental to all biochemical processes and an essential part of aerobic life metabolism [1]; whenever oxidative stress occurs in a living system, it may lead to cancer, diabetes, and cardiovascular diseases.

Cancer can engage any part of the body and has anatomic and molecular subtypes that each require specific management policies [2]. Cancer is the largest and second leading cause of death worldwide. In 2020, the number of death cases caused by cancer was about 10 million, or approximately one in six deaths. Deaths due to lung cancer were about 2.21 million [3]. Lung cancer is the major type of cancer and the best site for the metastasis process of tumors.

The various allopathic medicines for lung cancer treatments are gemcitabine, paclitaxel, docetaxel, etoposide, and vinorelbine [4]. Lung cancer, like all malignancies, has the best chance of being cured if diagnosed early in the disease's progression [5]. The most recurrent cancer in the world is lung cancer, with a prevalence of 6.3% and a death rate of 22.1% [3,6]. Tobacco smoking, secondhand tobacco smoke outflow (aloof smoking), line and stogie smoking, indoor and outside air contamination, atomic openness, nickel, chromium, and arsenic have been considered the causing agents for huge cases [7]. Tobacco use is the leading cause of lung cancer, and males are more likely than women to develop the disease [8]. Many medicinal plants were reported against various types of cancer, including lung cancer. As per the WHO survey, 80 % of the population in developed countries uses medicinal plants for basic illness and disease cures due to fewer side effects [9]. Modern allopathic medicine produces numerous side effects in cancer treatment. Researchers are searching for natural medicine with fewer side effects to overcome this problem for the treatment of cancer.

Many scientists have reported that *A. melanocarpa* has good potential to treat colorectal cancer, colon cancer, cardiovascular disease, chronic inflammation, gastric mucosal disorders (peptic ulcer), eye inflammation, and liver failure [10]. *Allium sativum*, *Curcuma longa*, *Momordicacharantia*, *Boerrhaviadiffusa*, *Stevia rebaudiana*, *Nelumbonucifera* and *Gymnemasylvestre* are effective for cancer treatment, especially for lung cancer treatment [11]. *Hygrophillaschulli* (M.R. Almeida & S.M. Almeida) is a medicinal plant that belongs to the Acanthaceae family and is widely distributed throughout India, Sri Lanka, Burma, Malaysia, and Nepal. The whole plant and ashes are widely used in various traditional medicine systems against diseases such as inflammation, jaundice, pain, urinary infections, hepatic syndromes, rheumatism, edema, and gout. This plant is also mentioned in the ayurvedic system as seethaveeryam and mathuravipaka for the treatment of prameham (Diabetes) and athisaram (Dysentery) etc. [12]. This study aimed to evaluate the phytochemical content of *H. schulli* leaves extracts and isolate the molecule responsible for the antioxidant and antiproliferative effects on the human lung cancer cell line (A549). However, the current research reports that phytomedicines and their plant-based phytochemicals may have fewer side effects as compared to synthetic drugs [13].

2. Materials and Methods

2.1. Collection of plant material and extraction.

Hygrophillaschulli was collected from Thanjavur, Tamil Nadu, and authenticated at the Botanical Survey of India, Coimbatore. The collected plants' leaves were washed in running tap water and rinsed with distilled water. They were dried at a temperature of 35° C away from light for 5 days before being reduced to powder using an electric grinder for the extractions. 200 g of *H. schulli* leaf powder was introduced into conical flasks with 200 ml of solvent: petroleum ether, ethyl acetate, chloroform, methanol, and ethanol. The mixture was stirred continuously in a stirrer for 24 h and then filtered through Whatman No. 1 filter paper (Yadav

et al. 2012). The filtrates were concentrated with a rotavapor, through which the dry extract was obtained about 15.25 g of yield.

2.2. Estimation of total phenolic content.

The total phenolic content of *H. schulli* leaves was determined to be a gallic acid equivalence [14]. The dried extracts were dissolved in the alcohol solvent at a concentration of 1 mg/ml, and a sample of 10 µl was drawn and transferred into a volumetric flask (10 ml). Then, 0.5 ml of Folin-Ciocalteu reagent was added and incubated for 10 min. After, 20% (w/v) prepared Na_2Co_3 (1.5 ml) was added and made up to 10 ml. The reaction mixture was incubated at 25 °C for 1 h, and the absorbance was read at 760 nm. Results were estimated in equivalence of Gallic acid (µg EqGA/mg of extract) used as standard.

2.3. Determination of total flavonoid content.

The total flavonoid content present in the extracts was checked according to the method described by Shraim *et al*., 2021 with some modifications [15]. The extract (µg/ml) was added to 0.1 ml of aluminum chloride (10%) and 0.1 ml of potassium acetate (1M), then kept at a temperature of 27°C for 30 min. The absorbance was read at 415 nm, and the total flavonoid contents of *H. schulli* leaves were estimated in Quercetin equivalence of extract (µg EqQ/ml of extract).

2.4. Estimation of total alkaloid content.

The total alkaloids present in *H. schulli* leaves were determined according to the method described by Shamsa *et al.* [16]. 1 mg of leaf extract was dissolved in alcohol, and 1 ml of Hydrochloric acid (2N) was filtered in the solution. That was transferred to a separating funnel; add 5 ml of bromocresol green and 5 ml sodium phosphate buffer. The mixture was shaken with 4 ml of chloroform by vigorous shaking, and that was collected in a volumetric flask and again diluted with chloroform up to the volume. The absorbance was measured at 470 nm. The standard was calibrated with caffeine, and total alkaloid content was assessed in equivalence of caffeine (mg EC/g of extract).

2.5. Antioxidant activity of H. schulli extracts.

2.5.1. DPPH radical scavenging activity.

DPPH radical scavenging activity was determined by the method described by Manochai *et al.* [17]. The reaction mixture for the test consists of 0.5 ml of samples, 3 ml of absolute ethanol, and 0.3 ml of DPPH radical solution (0.5 mM in ethanol). A mixture of 3.3 ml ethanol and 0.5 ml sample served as blank, and 3.5 ml ethanol and 0.3 ml DPPH radical solution was used as control. All the tubes were read at 517 nm after 1 h. The DPPH radical scavenging potential of the test sample was determined using the following formula.

$$\% \text{ of scavenging activity} = (OD_{control} - OD_{test})/OD_{control} \times 100$$

2.5.2. ABTS decolorization assay.

The *H. schulli* leaves extract was evaluated for its ABTS, and the radical capacity was analyzed. The stock solution contains ABTS solution (7mM) and 2.45mM potassium

persulphate. The working solution was prepared by adding the two solutions in equal quantities. The incubation was carried out for 12 h off from light. Then add 2 ml ABTS solution and allow to react for 7 min; then, the absorbance was measured at 750 nm.

% of scavenging activity= $(OD_{control} - OD_{test})/OD_{control} \times 100$

2.5.3. Determination of reducing power.

Various concentrations of the plant extracts (mg/ml) were mixed with 2 ml of phosphate buffer (0.2M, pH 6.7) and 2 ml of potassium ferricyanide (1%). The mixture was incubated for 25 min. 2 ml of trichloro acetic acid (10%) was added and then centrifuged at 3000rpm for 10 min. The supernatant (2.5 ml) was added to 2.5 ml of distilled water and 0.5 ml of ferric chloride; then, the absorbance was measured at 700 nm. A high absorbance value indicates a high reducing power. L-ascorbic acid was used as standard [18].

2.5.4. Nitric oxide radical scavenging activity.

0.5 ml extract in methanol was incubated with 3 ml Sodium nitroprusside (5 mM) in phosphate buffer at 25 °C for 30 min. 0.5 ml of PBS instead of the test sample was used as a control. After incubation, 1.5 ml Griess reagent (1% sulphanilamide, 2% H_3PO_4, and 0.1% naphthyl ethylene diaminedihydrochloride) was added to all the tubes and the absorbance was read at 546 nm as against the blank [11].

% of scavenging activity= $(OD_{control} - OD_{test})/OD_{control} \times 100$

2.6. In vitro cytotoxic potential of H. schulli and their active compounds

2.6.1. Cell treatment procedure.

The cell suspension was diluted with a medium containing 5% FBS to give a final density of $1x10^5$ cells/ml. 100 µl per cell suspension was seeded into 96-well plates at a plating density of 10,000 cells/well and incubated to allow for cell attachment at 37 °C, 5% CO2, 95% air, and 100% relative humidity. After 24 h the cells were treated with serial concentrations of the test samples. They were initially dispersed in DMSO and diluted to twice the desired final maximum test concentration with a serum-free medium. Aliquots of 100 µl of these different sample dilutions were added to the appropriate wells already containing 100 µl of the medium, resulting in the required final sample concentrations. Following the drug addition, the plates were incubated for 48 h at 37 °C, 5% CO2, 95% air, and 100% relative humidity. The medium containing samples was served as a control. *In vitro*, the anticancer activity of the isolated compound was performed as mentioned above. The following quantity of compound was tested: 6, 12, 25, 55, and 85 µl. All the experiments were performed in triplicate [19].

2.6.2. MTT assay.

After 48 h of incubation, 15 µl of MTT (5 mg/ml) in phosphate-buffered saline (PBS) was added to each well and incubated at 37 °C for 4 h. The medium with MTT was then flicked off, and the formed Formosan crystals were solubilized in 100 µl of DMSO. Then, the absorbance was measured at 570 nm using a microplate reader [19].

Percentage viability (%)=(Absorbance of test)/(Absorbance of control) x 100

A nonlinear regression graph was plotted between % Cell inhibition and Log concentration, and IC_{50} was determined using Graph Pad Prism software.

2.6.3. Flow cytometric analysis.

Cell cycle analysis was performed on the A549 cell line to determine the cell cycle arrest of the isolated fraction. The analysis procedure was done primarily by cell seeding in 6-well plates with a cell density of 2 x 10^5 cells. The cells were then treated with 6 µg/ml (low dose) and 12 µg/ml concentrations of isolated compound. The cells were trypsinized and centrifuged at 100 rpm for 10 min after incubation. Then, the cells were thrice washed with PBS, set to ice-cold ethanol at 70%, and deposited at 4 °C. After fixation, the cells were stained with 50 µl of propidium iodide and stored in a dark room at room temperature for 30 min. Then the cells were analyzed with a flow cytometer (BD AccuriTM C6, USA), and the flow jow program was used to determine cell cycle dispersion [20].

2.7. GC-MS Analysis.

Fractions from *H. schulli*, which contains 2-5 spots on TLC have been taken for GC-MS analysis to find phytochemical composition using GC-MS [21]. Analyses were carried out using Perkin Elmer-Clarus 500 with a capillary column directly coupled to the mass spectrometer system column (Elite-5ms) (30mx 0.25mm ID fused of 5% phenyl 95% dimethylpolysiloxane). Oven temperature 70ºC @ 6º C minutes to 170ºC (2 min) @ 6º C/min to 290ºC (5min); injector temperature 290ºC, carrier gas He, flow rate 1 ml/min; split ratio 1:10; mass spectral were taken ionization energy at 70ev, 200ºC, scanning.

2.8. Isolation and characterization of phytoconstituents from H. schulli leaves extract by column chromatography.

Column chromatography (CC) is the traditional method for isolating bioactive chemicals in a gradient ratio of organic solvents. The gradient solvent system was used for elution as per PE: EA (100:0-0:100; v:v), EA (100%), CH:ME (100:0-0:100), and ME (100%) combinations (v: v) in increased polarity ranges. Fractions were collected and distilled to remove excess solvents in separate glass tubes. Eluted aliquots were labeled with respect to the solvent system. Then, fractions were tested for the single homogenized spot by thin-layer chromatography (TLC) coated with the pre-activated (placed in a hot air oven) Silica gel (TLC grade) over a glass slide manually. 3-5 µl of collected fractions were placed 1 cm above the glass slide of the stationary phase in the appropriate combination of a solvent system (10:1–10: v: v). TLC plates were kept in the iodine chamber for unique single-spot identification [22]. The homogenized spot fractions were used directly in the spectral evaluation.

2.8.1.Spectral Studies.

UV-VIS Spectroscopy is a low-cost method of determining a compound's purity. The absorbance capacity was determined using an 800-200 nm wavelength for electronic transmission [23]. The functional groups in the isolated molecule are determined using Fourier Transform Infra Red (FT-IR) Spectral analysis. FT-IR makes it simple to identify and characterize chemical bonds within a sample. The isolated compound's functional group was discovered using the potassium bromide (KBr)-pelletizing process. The sample was combined with the KBr pressed into a pellet and subsequently analyzed. The bond type was determined

using FT-IR (Affinity-1, Shimadzu, Japan) at a wavelength spanning from 4000-400 cm-1 [24]. A single isolated compound was subjected to discovering protons and atoms to elucidate the putative skeletal structure verification. Protons are found using ^{1}H NMR, and the undefined sample matrix of carbon atoms is determined using ^{13}C NMR [25]. Signals detected in the ^{1}H and ^{13}C NMR spectrums were recorded by the 300MHz Bruker DR X to predict the structure of the isolated phytocompound [26].

2.9. Preparation of ligands and proteins.

Bioactive compounds from active fractions and isolated compounds were docked on cancer receptors using the Autodock software [27]. The receptors were selected based on diagnostic, predictive, and prognostic biomarkers obtained from the Protein Data Bank selected from predictive biomarker [28], BRAF (V-RAF murine sarcoma viral oncogene homolog B1) receptor complexed with PLX5568 selected from prognostic biomarker with PDB ID: 1m17 [29], the tumor suppressor protein of p53 cancer mutant Y200C selected from diagnostic biomarker with PDB ID. External complex ligands from the selected receptors were eliminated and ready to dock using Discovery Studio software by Scripts selection. The ligands of isolated and PPF compounds were extracted as a 3D SDF file from PubChem.

2.9.1. Molecular Docking

In the docking mode, ligands were individually uploaded in Autodock file format (3D SDF). After researching the receptor's unique binding region, the respective proteins for the molecular interaction were uploaded individually in protein mode. The receptor's binding site was selected based on the real protein binding site's amino acid residue position (auth). The binding pocket was also expanded to include an exterior binding site for amino acids. After docking, the Hide calculation of the individual ligands was performed to determine the binding interaction in picomolar to millimolar concentrations. Based on hide computation in the ECF file type, the best-docked ligands were chosen, followed by the docked protein in the pdb file format. The hydrogen bonds are then found in the best-docked file by visualizing amino acid residues in 2D and 3D structures for each ligand and receptor [30].

2.10. Statistical analyzes

The results were analyzed by the GraphPad software and then presented in the form of means ± errors. The treated groups were compared to the control, and the threshold for the significant difference was set at $P < 0.05$.

3. Results and Discussion

3.1. Estimation of total phenolic, flavonoid, and alkaloid contents from H. schulli leaves.

The phytochemical analysis of the leaf extracts of *H. schulli* revealed the presence of substantial amounts of phenols, flavonoids, and alkaloids.

The total phenolic content in *H. schulli* leaves extract was obtained using the Gallic acid linear curve. Figure 1A shows the total phenolic contents of the plant *H. schulli* leaves, which were 25.9 ± 0.98 µg/ml (HS-M), 20.3 ± 0.96 µg/ml (HS-E), 18.6 ± 1.01 µg/ml (HS-CH), 15.8 ± 1.04 µg/ml (HS-EA), 12.4 ± 0.85 µg/ml (HS-PE). The total phenolic content was high in methanolic extract compared to the other solvents. The total flavonoid content was obtained

using the regression calibration curve of quercetin. Figure 1B shows that extract of *H. schulli* leaves contains 28.75 ± 0.95 µg/ml (HS-M), 22.55 ± 0.79 µg/ml (HS-CH), 17.05 ± 0.96 µg/ml (HS-EA), 15.80 ± 0.95 µg/ml (HS-E), 12.76 ± 0.86 µg/ml (HS-PE) flavonoids in all these extracts. High amounts of flavonoids were found in methanolic extract compared to the other solvent extracts. The total alkaloid content in *H. schulli* leaves extract was obtained by using the curve of caffeine. Figure 1C shows that by using the caffeine linear curve, the total alkaloid contents in *H. schulli* leaves were 31.2 ± 1.02µg/ml (HS-CH), 26.5 ± 0.97µg/ml (HS-M), 23.5 ± 0.85µg/ml (HS-EA), 16.5 ± 0.92µg/ml (HS-E), 14.5 ± 0.94µg/ml (HS-PE) in all the solvent extracts. The total alkaloid content was high in chloroform leaf extract. The phytochemical analysis of the leaf extracts of *H. schulli* revealed the presence of alkaloid, phenolic, and flavonoid compounds. These are a large group of phytochemicals that might probably account for the therapeutic and pharmacological properties of *H. schulli* leaves. These phytoconstituents are reported to act as primary antioxidants and thus employ several free radicals to determine their radical scavenging activity. The high content of total alkaloids in the chloroform extract compared to the other extracts was in agreement with the results obtained by Parthasarathy *et al.* [31]. Phenolics and flavonoids are the primary group of lead molecules that will act as natural antioxidants in human diets; therefore, the estimation of these active phytoconstituents was performed. Comparatively, the methanol extract of *H. schulli* leaves contains a high level of phenolics and flavonoids. Similar results were observed in Barlerianoctiflora [32].

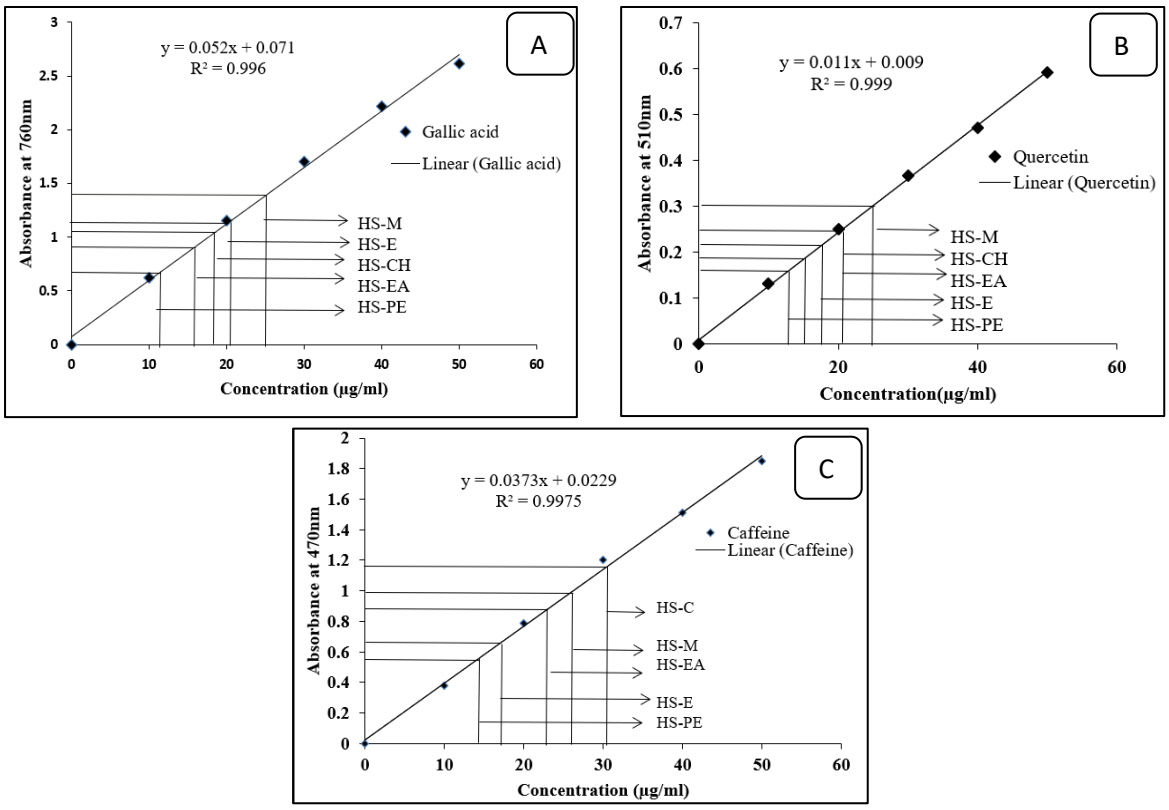

Figure 1. Estimation of total phenolic (A), flavonoid (B), and alkaloid (C) content in Hygrophilaschullileaf extracts. HS-M (methanolic extract), HS-E (ethanolic extract), HS-CH (chloroform extract), HS-EA (ethyl acetate extract), HS-PE (petroleum ether extract)

3.2. Determination of antioxidant activities of H. schulli leaves.

The ability of *H. schulli* leaves to scavenge free radicals and their consequent redox properties was scrutinized using DPPH assay, ABTS cation decolorization assay, and ferrous

reducing power assay. The results obtained revealed that the reduction capacity of DPPH radicals was determined by the decrease in the absorbance at 517 nm. The IC_{50} value of the standard antioxidant (L-ascorbic acid) was 30.9 ± 1.04 µg/ml. For methanolic extract, it was 75.75 ± 1.03 µg/ml, and for other extracts, they were above 100 µg/ml (Figure 2A). The lower IC_{50} value indicates the higher radical scavenging activity of the extracts. The results show that the methanol extract of *H. schulli* has more ability to scavenge free radicals generated by DPPH. ABTS cation decolorization assay was performed in the extracts (Figure 2B). It was observed that the IC_{50} value of the standard antioxidant (L-ascorbic acid) was 26.9 ± 0.95 µg/ml, for methanolic extract 65.75 ± 0.86 µg/ml, chloroform extract 80.6 ± 0.79 µg/ml and other extracts were above 100 µg/ml. The lower IC_{50} value indicates higher radical scavenging activity. The methanol extract of *H. schulli* contains high activity compared to the other extracts. Nitric oxide radical scavenging assay displayed that the IC_{50} value of the standard antioxidant (L-ascorbic acid) was 20.9 ± 0.59 µg/ml and 59.75 ± 0.76 µg/ml for methanolic of *H. schulli*, for chloroform extract 79.6 ± 0.98 µg/ml and other extracts was above 100 µg/ml (Figure 2C). The lower IC_{50} value indicates higher radical scavenging activity. Ferrous reducing power assay suggested that the increasing absorbance of the reaction mixture indicates a higher antioxidant capacity (Figure 2D). The results showed that the methanolic extract had a high increasing absorbance compared to the other solvent extracts. This high antioxidant activity of phenolic and flavonoid compounds was also observed in methanolic extract of Thymus daenensisCelak, Saturejabachtiarica Bung., DracocephalummulticauleMontbr& Auch and Stachys lavandulifoliaVahl. by GhasemiPirbalouti *et al*. [33]. Other authors had previously proved the antioxidant activity of phenolic and flavonoid compounds in the extracts of certain plants. Phenolic compounds from *Rosmarinus officinalis* and *Thottea siliquosa* extracts possess good antioxidant activity [34,35].

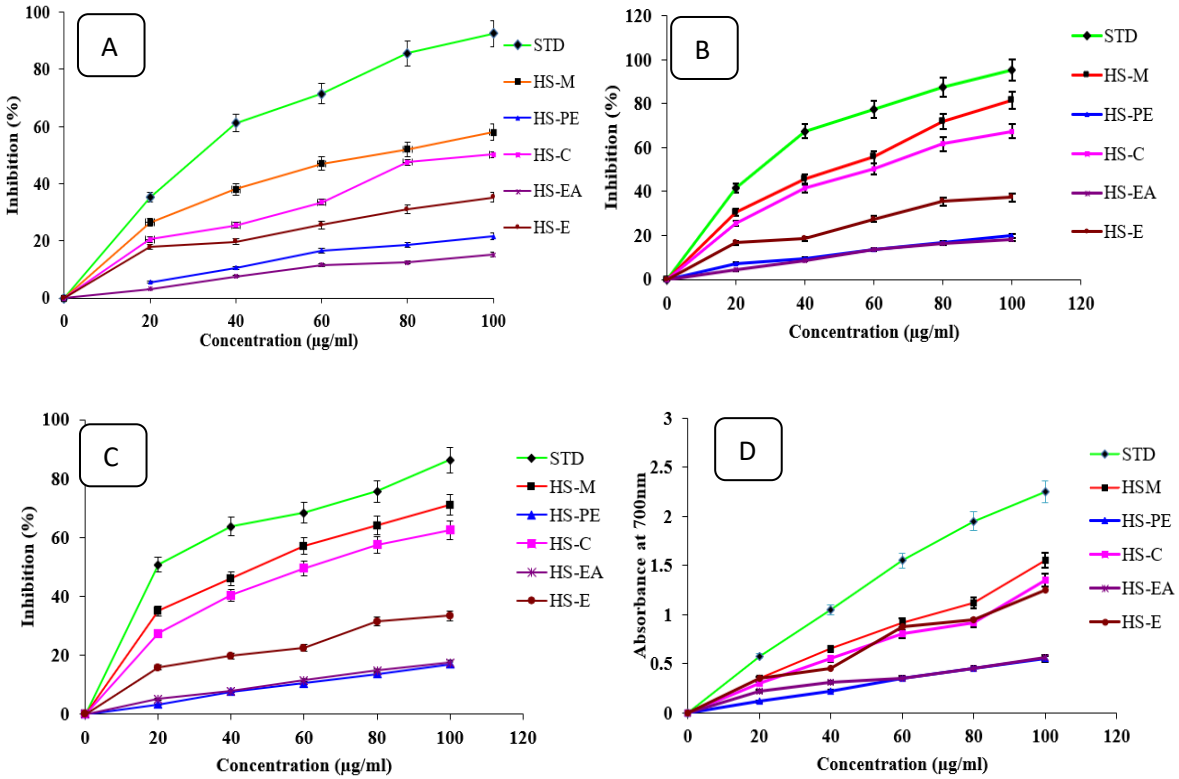

Figure 2. DPPH free radical scavenging activity **(A)** ; ABTS cationdecolourisation assay **(B);** Nitric oxide radical scavenging activity **(C)** ; and Ferrous reducing power activity **(D)** of *Hygrophilaschulli*leaf extracts.

3.3. Antiproliferative potential of active molecules from H. schulli extracts.

MTT assay was performed to examine the anticancer activity of the plant extracts against the human A549 lung cancer cell line. As shown in Figure 3A, the IC_{50} value of the standard doxorubicin was 30.9 ± 0.58 µg/ml, and for chloroform extract, 35.6 ± 0.45µg/ml, 45.75 ± 0.55 µg/ml for methanolic of *H. schulli*, and other extracts are 41.9 ± 0.85 µg/ml for HS (E), 49.6 ± 0.75 µg/ml for HS (EA). The lower IC_{50} value indicates higher anticancer activity. The results revealed that the chloroform extract of *H. schulli* possessed more anticancer properties. Figures 3B, C, and D showed the morphological response of A549 cells treated with the standard drug doxorubicin and chloroform extract of 6 and 12 µl, respectively. The MTT and Flow cytometric analyses revealed that the chloroform extract possesses the *in vitro* anticancer activity. The morphological response of A549 cells was obtained after treatment with chloroform extract and standard drug doxorubicin. The cytotoxic potential undertaken by Sufian and Haque in the brine shrimp lethality bioassay revealed that the extract of *H. schulli* possessed significant cytotoxicity (LC_{50} = 0.1 µg/mL) [36]. The *in vitro* antioxidant and anticancer activities of chloroform extracts of *H. schulli* leaves can be due to the presence of secondary metabolites. Then, these findings were subjected to isolating each bioactive compound in the extract to evaluate the accurate mechanism of action for lung cancer treatment.

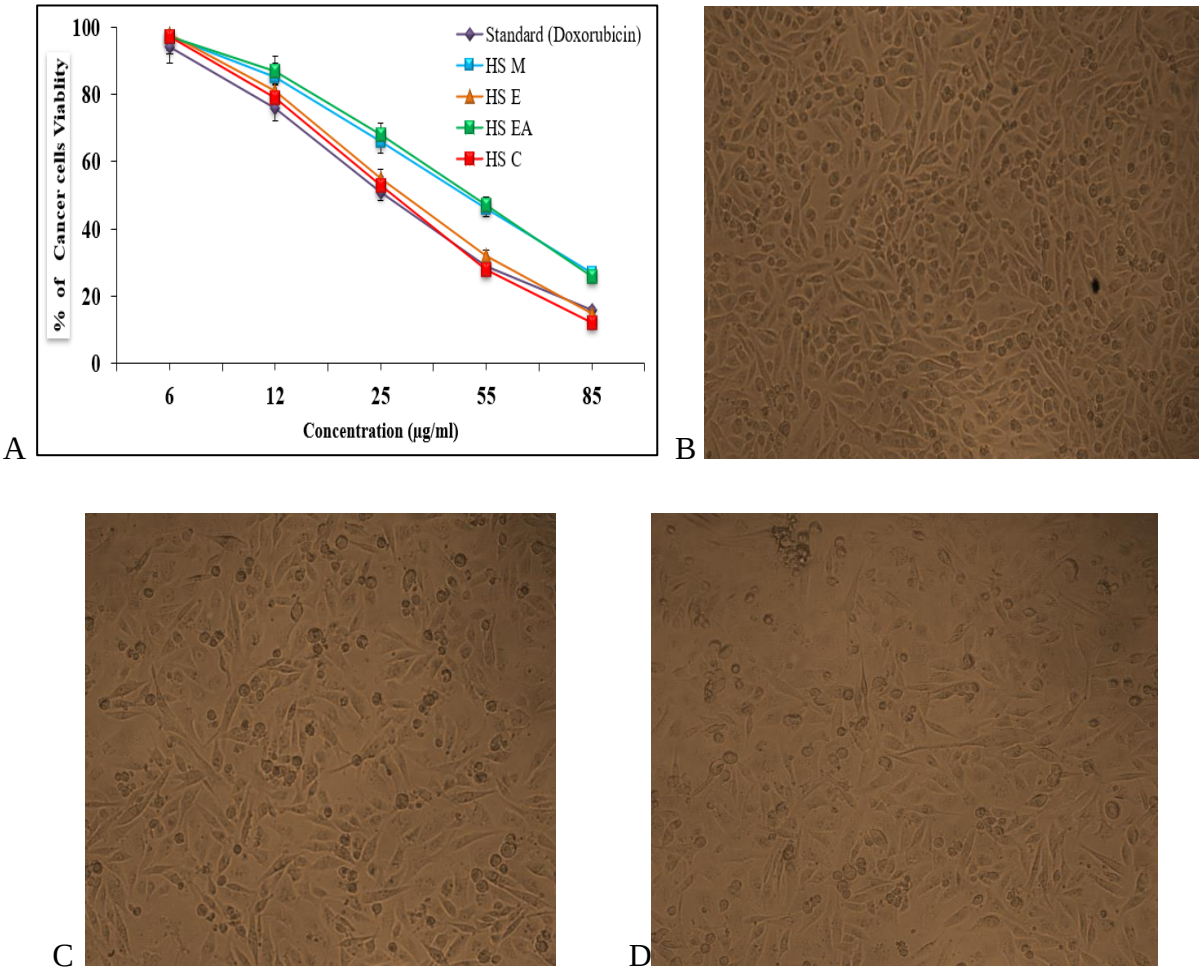

Figure 3. Percentage of inhibition of cancer cells by the extracts of Hygrophilaschullileaves **(A)**. HS-M (methanolic extract), HS-E (ethanolic extract), HS-C (chloroform extract), HS-EA (ethyl acetate extract), HS-PE (petroleum ether extract). Morphological response of A549 cells against control standard drug Doxorubicin (B), 6µl (C), and 12µl of chloroform extract of HS leaves. Magnification: 100X. Scale bar: 100µm.

3.4. GC-MS analysis of chloroform extract of H. schulli leaves.

The chloroform extract of *H. schulli* has more antioxidant and cytotoxic potentials than other solvent extracts. Further, the chloroform extract was analyzed by Gas chromatography and mass spectrum to identify the volatile molecules present in the extract. Chromatogram peaks were fallen within the retention time range from 03:12.1 (minutes: second) to 29:24.3 (minutes: second) (Supplementary Figure S1). Molecules were identified using the KI value from the National Center for Biotechnology Information database (Supplementary Table S1).

Consequently, a broad range of phytochemical compounds was identified from the chloroform extracts of *H. schulli* leaves through the GC-MS analysis. The identification of the phytochemical compounds was confirmed based on peak area and retention time.

3.5. Isolation and characterization of phytomolecules from the chloroform extract of H. schulli leaves.

The methanolic extract was used separately by liquid-liquid extraction with polar order and subjected to thin-layer chromatography for the purity of fractions (Table 1). The resolution of the fractions was very good. It was found that the 5th fraction of the 8:2 petroleum ether and ethyl acetate solvent system displayed a single spot with the Rf value of 0.82.

Table 1. TLC profile of isolated fractions from chloroform extract of *H. schulli* leaves.

Eluting solvents	Fractions	solvent systems	No. of spots	Color of spot	R_f Value
100% peth	1-7	100% peth	-	-	-
80:20 peth:AcOEt	1-10	8:1 peth:AcOEt	1(5^{th})	Yellow	0.82
50:50 peth:AcOEt	1-10	8:2 peth:AcOEt	2	Dark green	0.52,0.42
100% AcOEt	1-10	9.5:0.5 chl:MeOH	4	Green	0.72,0.88,0.97,0.94
100% chl	1-9	5:5 chl:MeOH	2	Green	0.15,0.31
80:20 chl:MeOH	1-7	8:2 CH:ME	2	Dark green	0.68.0.57
50:50 chl:MeOH	1-11	9:1 chl:MeOH	3	Pale green	0.72,0.80
100% MeOH	1-6	2:8 chl:MeOH	-	-	-

peth : petroleum ether; AcOEt: ethyl acetate; chl : chloroform; MeOH: methanol; EtOH: ethanol.

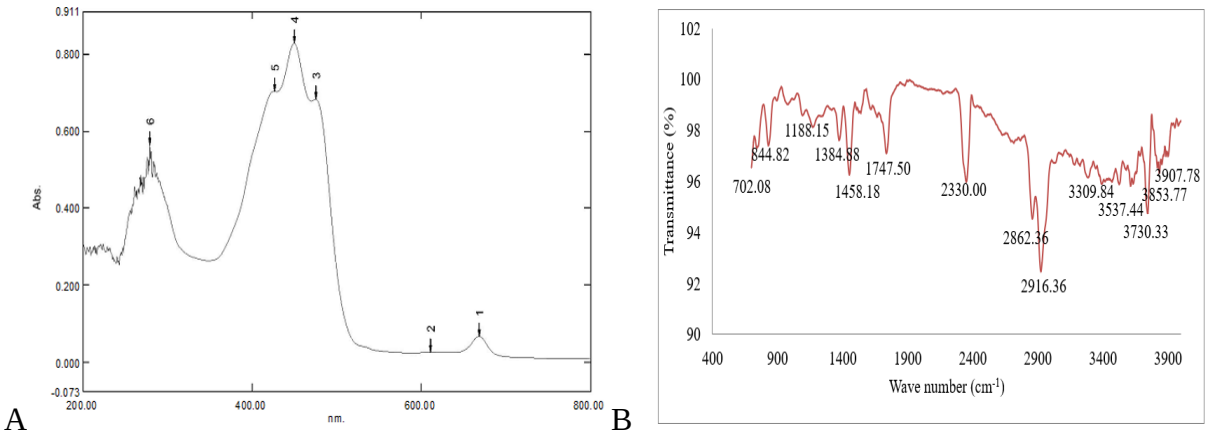

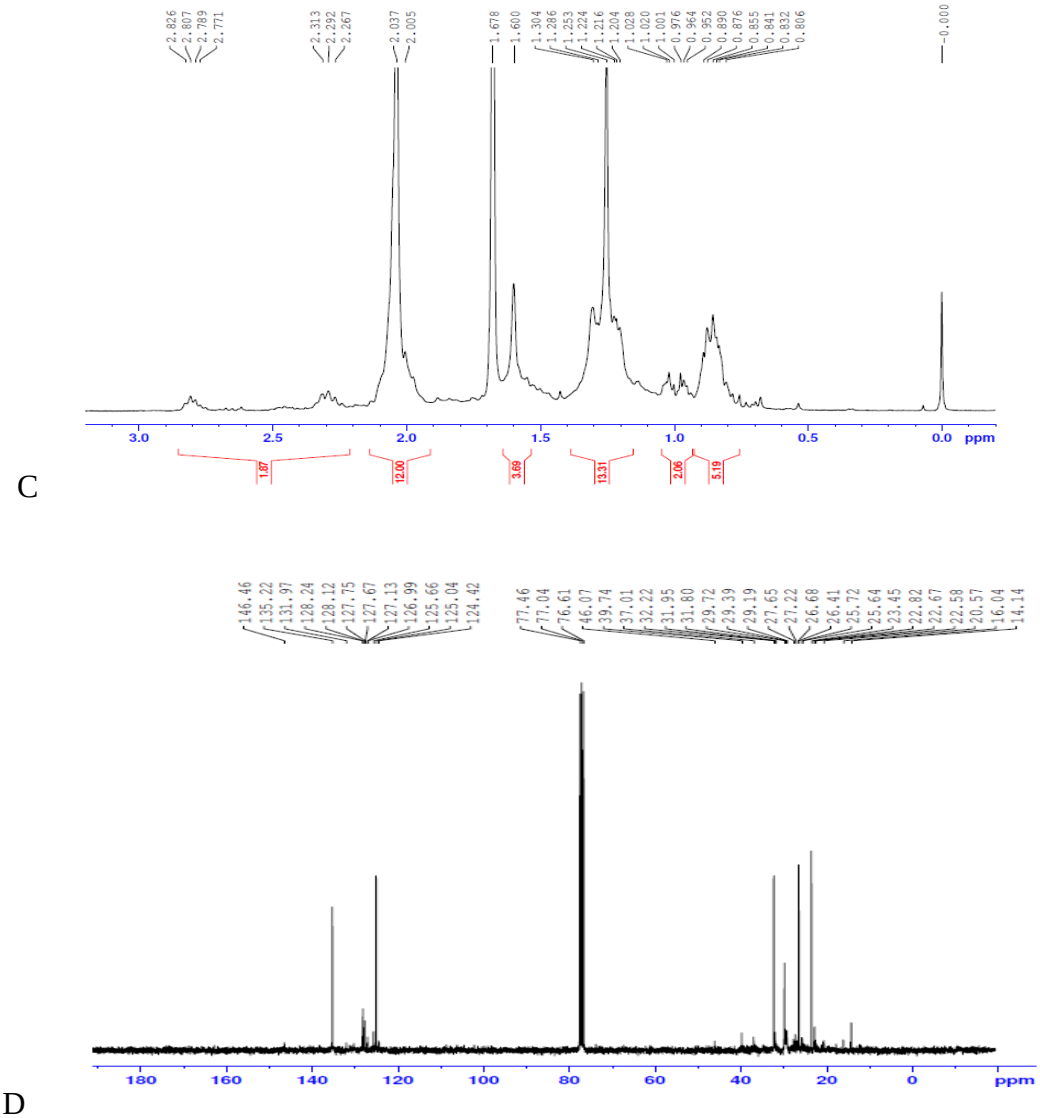

Figure 4. (A) UV-Visible spectrum of isolated fraction from Hygrophilaschullifraction 5 (8:2 Petroleum ether and Ethyl acetate); **(B)** Fourier Transform Infra-Red (FTIR) spectroscopy of the isolated fraction5 (8:2 Petroleum ether and Ethyl acetate); **(C)** ^{1}H-NMR Spectrum of the isolated compound to analyze the total number of protons present in the compound (Expanded view); **(D)** ^{13}C-NMR Spectrum of the isolated compound to analyze the total number of carbon atoms presents in the compound (Expanded view).

The isolated fraction was taken for further structural characterization using various spectral studies. UV-visible spectra of the isolated compound (5th fraction) were observed and found at 250 nm (Figure 4A) by using UV-Vis-Spectral data (UV-Vis-2450: Shimadzu, Japan). The maximum absorbance band was observed between 200-800 nm.FT-IR spectra of the isolated phyto-compounds from *H. schulli* were analyzed using a Shimadzu FT-IR spectrophotometer 400-4000 cm^{-1}. The FT-IR spectrum of the isolated compound was recorded and found the broadband at 3383 cm-1 indicated the presence of functional group O-H, the band at 1728 cm^{-1} due to carbonyl (C=O), and the absorption band at 1635 cm^{-1} is due to C=C group. The band at 1072 cm^{-1} indicates the ester (C-O) functional group (Figure 4B). ^{1}H-NMR spectrum was performed to find the presence of proton atoms in the isolated fraction. The signal at δ 0.806 indicated the presence of methyl group. The strong signal at δ 1.67 suggested that few methyl groups are attached to the unsaturated carbons. The strong signal at δ 2.03 suggested the presence of an allelic methylone group. The strong signal at δ 1.21 indicated the presence of a methylene group in a chain. The multiple signals at δ 5.12 showed the presence of unsaturated protons (Figure 4C). ^{13}C-NMR spectra showed the signals at δ 22.67 and 25.72 are due to methyl carbons attached to unsaturated systems. The signal at δ 29.39 and 31.95 is due to methylone carbons attached to an unsaturated system. The signal between δ 124.42 and 135.22 is due to unsaturated carbon atoms (Figure 4D). The above data suggest that few isoprene units are linked to each other. Based on proton NMR and carbon NMR and their signals, the structure and name of the molecule arrived tentatively as (5E,9Z,13Z)-2, 6, 10, 14, 18-pentamethylnonadeca-1, 5, 9, 13, 17-pentaene (328.57 g/mol).

3.6. Structure and the description of the isolated compound.

The structure of the isolated compound was identified from the chloroform extracts of *H. schulli* leaves. The isolated molecule was found to be (5E, 9Z, 13Z)-2, 6, 10, 14, 18-pentamethylnonadeca-1, 5, 9, 13, 17-pentaene (C24H40), which belongs to the family of steroids (Figure 5). The observation of UV -visible spectra of the isolated compound at 250 nm was in accordance with UV-spectroscopic results obtained by Patle *et al*. in Dilleniapentagyna [22]. The recorded FT-IR spectrum of the isolated compound showed that the band at 1072 cm-1 indicates the presence of an ester (C-O) functional group. Similar results were observed in FTIR spectral of *Hybanthus enneaspermus* by Anand *et al*., (2012) [37].

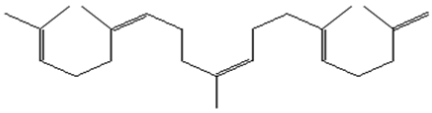

Compound name & Molecular formula	(5E, 9Z, 13Z)-2, 6, 10, 14, 18-pentamethylnonadeca-1, 5, 9, 13, 17-pentaene ($C_{24}H_{40}$)
Empirical formula	$C_{24}H_{40}$
Molecular weight	328.57
Exact mass	328.31
C log P	10.32
Log P	7.76

Figure 5. Description of isolated compound: (5E, 9Z, 13Z)-2, 6, 10, 14, 18-pentamethylnonadeca-1, 5, 9, 13, 17-pentaene.

Based on proton NMR and carbon NMR and their signals, the structure and name of the molecule arrived tentatively as (5E,9Z,13Z)-2, 6, 10, 14, 18-pentamethylnonadeca-1, 5, 9,

13, 17-pentaene (328.57g/mol). This deduction was also made by AbdGhafar *et al*. when they studied the NMR spectra of *Phyllanthus acidus* [38]. Finally, the structure of the isolated compound was identified from the chloroform extracts of *H. schulli* leaves and was found to be (5E, 9Z, 13Z)-2, 6, 10, 14, 18-pentamethylnonadeca-1, 5, 9, 13, 17-pentaene (C24H40), which belongs to the family of steroids.

3.7. Antioxidant and anticancer activity of the isolated molecule.

DPPH free radical scavenging activity showed a higher reduction of synthetic radical DPPH with an IC_{50} value of 57.6 ± 0.844 µg/ml and followed the IC_{50} value found at 32.8 ± 0.951µg/ml for the L-ascorbic acid (Figure 6A). This shows the isolated molecule ((5E, 9Z, 13Z)-2, 6, 10, 14, 18-pentamethylnonadeca-1, 5, 9, 13, 17-pentaene) from the chloroform extract of *H. schulli* leaves contain the higher antioxidant capacity and produce 80% inhibition approximately with 100 µg/ml concentration. ABTS decolorization assay revealed that the IC_{50} value for the isolated molecule and L-ascorbic acid was 55.8 ± 0.862 µg/ml and 22.3 ± 0.75µg/ml, respectively (Figure 6B).

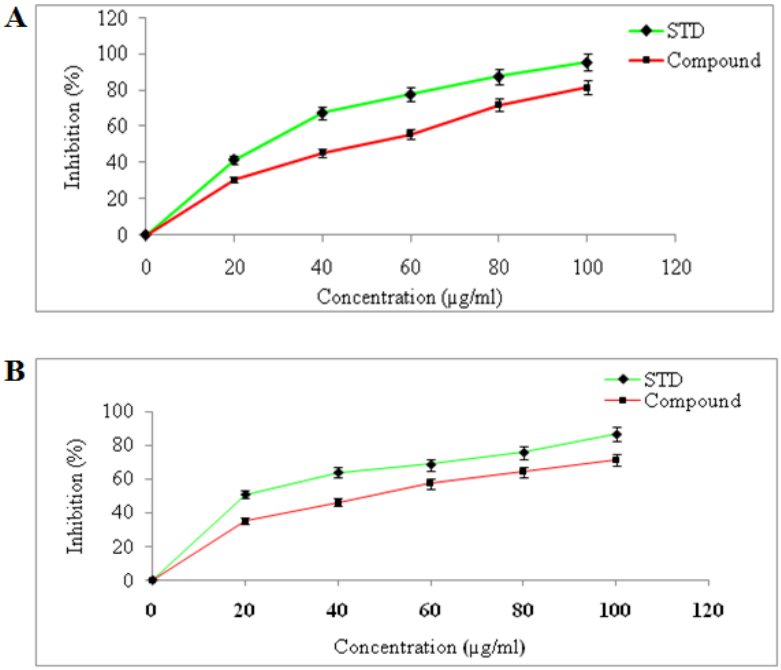

Figure 6. (A) DPPH free radical scavenging activity (STD- is the standard ascorbic acid); **(B)** ABTS assay (STD- is the standard ascorbic acid).

The antiproliferative potential of isolated fraction ((5E, 9Z, 13Z)-2, 6, 10, 14, 18-pentamethylnonadeca-1, 5, 9, 13, 17-pentaene) was determined by MTT assay on lung cancer cell line (A549) using different concentration (Figure 7). The extract and fraction showed dose-dependent inhibition of cell proliferation in the lung cancer cell line. The percentage of viability of the cells treated with 6, 12, 25, 55, and 85 µl of the isolated compound is (5E, 9Z, 13Z)-2, 6, 10, 14, 18-pentamethylnonadeca-1, 5, 9, 13, 17-pentaene. High activity was observed for the isolated fraction of the plant. The isolated fraction showed high activity towards the A549 cancer cell line, where the standard is also compared in the figures below.

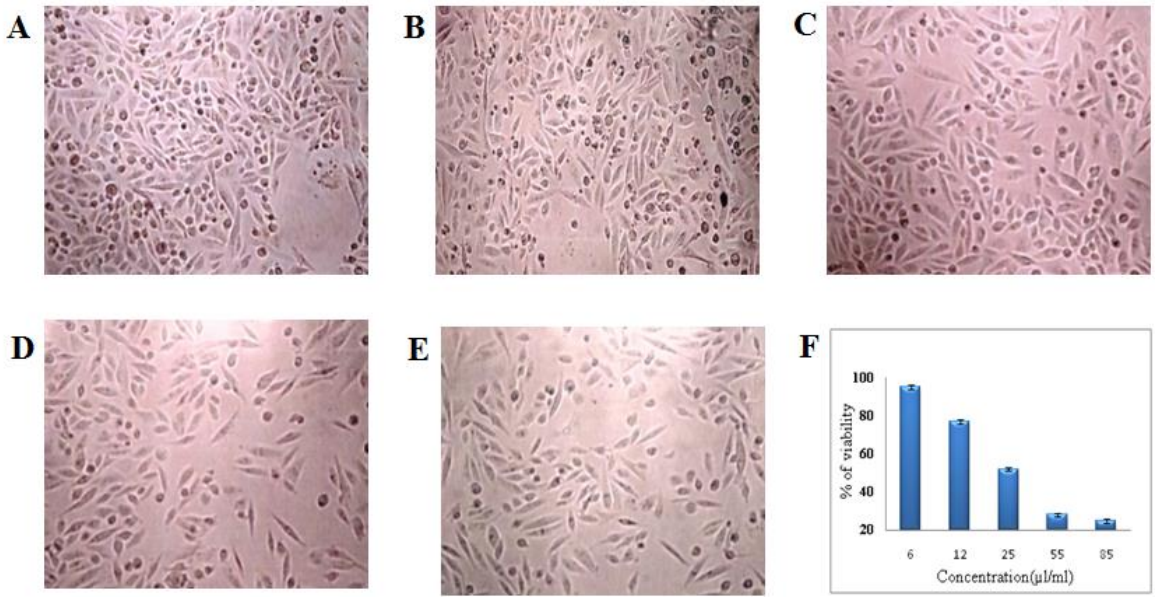

Figure 7. (A) 6µl of isolated compound on A-549 cells; **(B)** 12µl; **(C)** 25µl; **(D)** 55µl and **(E)** 85µl of isolated compound on A-549 cancer cell lines with 100x magnification. F) Percentage of the antiproliferative ability of isolated molecules against cancer cells.

3.8. Cell cycle arrest of the isolated molecule.

Flow cytometric analysis revealed that the isolated fraction induced cell cycle arrest at the G2/M phase (Figure 8A, B, C, and D). Treatment with the isolated fraction at a low dose 6 µg/ml, medium dose of 12 µg/ml, and high IC_{50} dose shifted the population of A549 cells into the G2/M phase from the G1 phase. At 6 µg/ml, 2% of cells were in the G2/M phase, while at 12 µg/ml, cells in the G2/M phase were increased to 3% with a reduced number of cells at the G1 phase as compared to the control (Figure 8E).

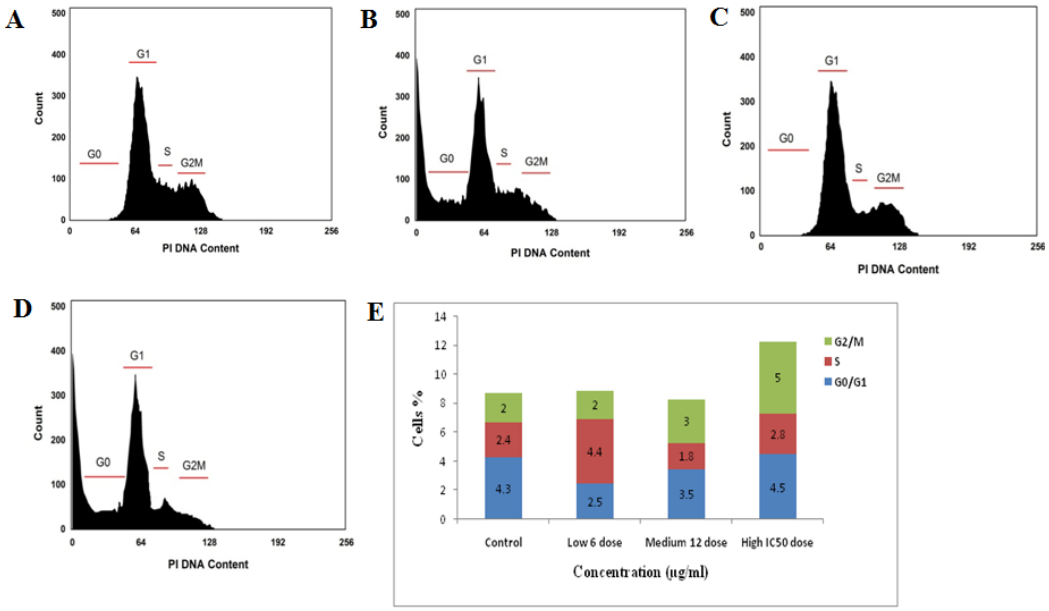

Figure 8. (A-D) Fraction-induced cell cycle arrest in A-549 cancer cells analyzed by flow cytometry. A-549 cells were treated with DMSO (Control), isolated compounds with 6 low doses, 12 medium doses, and high IC_{50} doses for 48 hours. The cells were fixed, stained with propidium iodide, and analyzed by flow cytometry. E) The graph shows the percentage of A-549 cells in different phases of the cell cycle on incubation with the isolated compound at 6 µg/ml, 12 µg/ml and high IC_{50} dose for 48 hours as analyzed by flow cytometry.

The proportion of cells in the G1 and S phases decreased, while there was a marginal increase in the cells in the G2/M phase. These results signify that the isolated fraction from the *H. schulli* leaves efficiently induces cell cycle arrest at the G2/M phase in a dose-dependent manner, further demonstrating the cell cycle regulation and consequent inhibition of lung cancer cell proliferation.

3.9. In silico molecular docking of the phytomolecule from the H. schulli on EGFR receptor.

Molecular recognition is a basic requisite for the prediction and investigation of the molecular basis of a particular compound. Our study relied on the docking simulation of the isolated compound of *H. schulli* (ligand) on EGFR receptor (target protein). The compounds showed high binding energies with EGFR ranging from -7.0. The compound established a network of molecular interactions (H-bonds, Van der Waals (VdW), alkyl, π-alkyl, and π-sigma bonds) with the active-site residues of EGFR when analyzed in 2D plots. Molecular interaction and their 2D files for doxorubicin and isolated molecules from *H. schulli* are given in Figures 9A and B and Figures 9 C and D, respectively. Isolated molecule and doxorubicin showed interaction with EGFR receptors. The connection between the ligand and receptor with aspartic acid and threonine amino acid residue (A:872) and Thr (A:879) followed -7.0 and -8.3 binding energy, respectively (Table 2). Thus, docking studies revealed that the ligand interacts with the protein with high binding affinities.

Table 1. Molecular docking studies of isolated molecules from chloroform extract of *H.schulli* leaves and Doxorubicin on EGFR.

No	Name of the molecule	Molecular weight	N.of hydrogen bond & length	Glide energy	Interacted amino acid residues
1	Molecule:(5E,9Z,13Z)-2,6,10,14,18-pentamethylnonadeca-1,5,9,13,17-pentaene	328.57g/mol	-	-7.0	Asp(A:872)
2	Standard: Doxorubicin	543.52g/mol	3Hbonds(2.2Å,2.1Å,2.3Å)	-8.3	Asp(A:872) Thr(A:879) Asp(A:872)

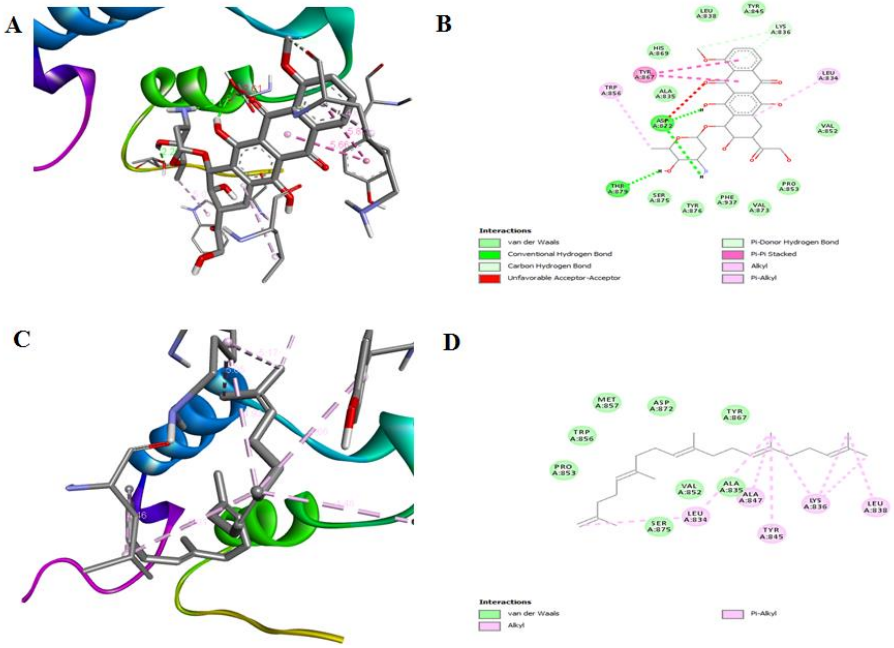

Figure 9. (A) and **(B)** Molecular interaction of standard (Doxorubicin) on EGFR and its 2D file; **(C)** and **(D)** Molecular interaction of isolated molecule on EGFR and its 2D file.

There are for the anticancer activity of the steroids from various plants. Steroidals from Dioscoreazingiberensis Wright (DZW) have shown cytotoxic activity in cancer cells [39]. Then, the isolated molecules from the chloroform extract of *H. schulli* leaves were further subjected to various screenings for antioxidant and anticancer activities. The results obtained from the antioxidant assays revealed that the isolated compound is a potent antioxidant. The high radical scavenging activity is predicted to be contributed by the functional groups such as hydroxyl groups, carbonyl keto groups, and conjugated double bonds present in the isolated compound by triggering redox reactions and thereby stabilizing the free radicals by donating hydrogen atoms. The DPPH free radical scavenging assay result was supported by the results of DPPH assay of protective and antioxidant effects of *H. schulli* seeds by Islam *et al.* [40].

This new pentaene also showed a good *in vitro* anticancer activity. The bioactive constituents of the reported isolated compound could be a prime cause for the significant cytotoxic activity in A549 cell lines by altering its tumor survival characteristics. These results were similar to those seen by Satpathy *et al*. when studying the green synthesis of gold nanoparticles mediated by extract of Hygrophilaspinosa [41]. Hence, the induction of cell cycle arrest by the isolated compound indicates that it is a prominent antitumor agent by blocking the G2/M phase transition. A similar trend has been observed in platinum nanoparticles in human cervical cancer cells by Alshatwi *et al.* [42]. Thus, docking studies revealed that the ligand interacts with the protein with high binding affinities. This indicates that the isolated compound has good efficiency to be screened as a potential phytomedicine against cancer by blocking the EFGR receptor, thereby inhibiting the proliferation and division of lung cancer cells. Similar results were obtained in silico molecular modeling and docking of allicin, epigallocatechin-3-gallate, and gingerol against colon cancer cell proteins by Elengoe *et al.* [43]. This study demonstrated the chloroform extract of *H. schulli* leaves possessed good *in vitro* antioxidant and anticancer potentials that were attributed to phytochemical from steroids family: $C_{24}H_{40}$, (5E, 9Z, 13Z)-2, 6, 10, 14, 18-pentamethylnonadeca-1, 5, 9, 13, 17-pentaene.

4. Conclusions

In the current scenario, the need for the best anticancer agents should be noted. But our drug discovery system fails to achieve that goal. In recent days, much scientific research and investigations have been going with the base of phytoremedies in order to prevent the side effects of modern synthetic medicines. The points that are combined with such investigations are one plant for many diseases, fewer adverse effects, and more effectiveness. Such a conclusion should lead the pharmaceutical industries to focus on plant-based medicines with large-scale production and sales. The active fraction was eluted and isolated from chloroform extract of *Hygrophila schulli* leaves based on the spectral data the molecule name derived as (5E,9Z,13Z)-2,6,10,14,18-pentamethylnonadeca-1,5,9,13,17-pentaene. The isolated molecule was screened against the lung cancer cell line (A549) and found to have a higher inhibitory effect. The current research explains the study of *in vitro* antioxidant and anticancer activity of *H. schulli* leaves and their novel phyto-bioactive molecule as a base for the drug discovery fields.

Funding

This research was funded by DST-FIST (SR/FST/LS-1/2018/187); DST-SHRI (DST/TDT/SHRI/2022/70) to complete this research work.

Acknowledgments

The authors are grateful to the Karpagam Academy of Higher Education for providing a laboratory to carry out research work.

Conflicts of Interest

The authors declare no conflict of interest

References

1. Winterbourn, C.C. Biological chemistry of superoxide radicals. *Chem Texts* **2020**, *6*, 1-13, https://doi.org/10.1007/s40828-019-0101-8.
2. Pisoschi, A.M.; Pop, A.; Iordache, F.; Stanca, L.; Predoi, G.; Serban, A.I. Oxidative stress mitigation by antioxidants-an overview on their chemistry and influences on health status. *Eur J Med Chem* **2021**, *209*, 112891, https://doi.org/10.1016/j.ejmech.2020.112891.
3. Cancer - WHO | World Health Organization. 3 February **2022**, https://www.who.int/news-room/fact-sheets/detail/cancer.
4. Nerkar, A.G.; Chakraborthy, G.S.; Ukirde, R.D. Anticancer agents from natural sources: A review. *Curr Trends Pharm Pharm Chem* **2021**, *3*, 38-46, https://doi.org/10.18231/j.ctppc.2021.011.
5. Rudin, C.M.; Brambilla, E.; Faivre-Finn, C.; Sage, J. Small-cell lung cancer. *Nat Rev Dis Primers* **2021**, *7*, 1-20. https://doi.org/10.1038/s41572-020-00235-0.
6. Cao, M.; Chen, W. Epidemiology of lung cancer in China. *Thorac. cancer* **2019**, *10*, 3-7. https://doi.org/10.1111/1759-7714.12916.
7. Alberg, A.J.; Brock, M.V.; Ford, J.G.; Samet, J.M.; Spivack, S.D. Epidemiology of lung cancer: Diagnosis and management of lung cancer: American College of Chest Physicians evidence-based clinical practice guidelines. *Chest* **2013**, *143*, e1S-e29S, https://doi.org/10.1378/chest.12-2345.
8. Ragavan, M.; Patel, M.I. The evolving landscape of sex-based differences in lung cancer: a distinct disease in women. *Eur Respir Rev* **2022**, *31*, https://doi.org/10.1183/16000617.0100-2021.
9. World Health Organization. WHO traditional medicine strategy: 2014-2023, World Health Organization, **2013**, https://apps.who.int/iris/handle/10665/92455.
10. Malik, M.; Zhao, C.; Schoene, N.; Guisti, M.M.; Moyer, M.P.; Magnuson, B.A. Anthocyanin rich extract from *Aronia meloncarpa* E. induces a cell cycle block in colon cancer but not normal colonic cells. *Nut. Cancer* **2003**, *46*,186-196, https://doi.org/10.1207/S15327914NC4602_12.
11. Shukla, V.K.; Doyon, Y.; Miller, J.C.; De Kelver, R.C.; Moehle, E,A,; Worden, S.E.; Mitchell, J.C.; Arnold, N.L.; Gopalan, S.; Meng, X.; Choi, V.M.; Rock, J.M.; Wu, Y.Y.; Katibah, G.E.; Zhifang, G.; McCaskill, D.; Simpson, M.A.; Blakeslee, B.; Greenwalt, S.A.; Butler, H.J.; Hinkley, S.J.; Zhang, L.; Rebar, E.J.; Gregory, P.D.; Urnov, F.D. Precise genome modification in the crop species Zea mays using zinc-finger nucleases. *Nature* **2009**, *459*, 437-441, https://doi.org/10.1038/nature07992.
12. Fabricant, D.S.; Norman, R.F. The Value of Plants Used in Traditional Medicine for Drug Discovery. *Environ. Health Perspect.* **2001**, *109*, 69-75, https://doi.org/10.1289/ehp.01109s169.
13. Thirugnanasambandan, T.; Gopinath, S.C. Nanoparticles from plant-based materials: a promising value-added green synthesis for antidiabetic. *Biomass Convers Biorefin* **2022**, 1-11, https://link.springer.com/article/10.1007/s13399-022-03632-5.
14. Singleton, V.L.; Orthofer, R.; Lamuela-Raventós, R.M. Analysis of total phenols and other oxidation substrates and antioxidants by means of folin-ciocalteu reagent. *Methods Enzymol* **1999**, *299*, 152-178, https://doi.org/10.1016/S0076-6879(99)99017-1.
15. Shraim, A.M.; Ahmed, T.A.; Rahman, M.M.; Hijji, Y.M. Determination of total flavonoid content by aluminum chloride assay: A critical evaluation. *LWT*, **2021**; *150*, 111932, https://doi.org/10.1016/j.lwt.2021.111932.
16. Shamsa, F.; Monsef, H.R.; Ghamooshi R. Verdian R.M.R. Spectrophotometric Determination of Total Alkaloids in *Peganum harmala* L. Using Bromocresol Green. *Res J Phytochem* **2007**, *1*, *79-82*, https://scialert.net/abstract/?doi=rjphyto.2007.79.82.

17. Manochai, B.; Ingkasupart, P.; Lee, S.H.; Hong, J.H. Evaluation of antioxidant activities, total phenolic content (TPC), and total catechin content (TCC) of 10 sugar apple (*Annona squamosa* L.) cultivar peels grown in Thailand. *Food Sci. Technol*. **2018**, *38*, 294-300, https://doi.org/10.1590/fst.22117.
18. Cheng, Z.; Li, Y. Reducing power: the measure of antioxidant activities of reductant compounds?. *Redox Rep* **2004**, *9*, 213-217. https://doi.org/10.1179/135100004225005994.
19. Ghasemi, M.; Turnbull, T.; Sebastian, S.; Kempson, I. The MTT assay: utility, limitations, pitfalls, and interpretation in bulk and single-cell analysis. *Int J Mol Sci* **2021**, *22*, 12827, https://doi.org/10.3390/ijms222312827.
20. Manoharan, S.P.; Yadav, S.A.; Pandiyan, B.; Suvathika, G. Tragiaplukenetii-Assisted Omega-Decenol as Potential Anticancer Agent: its Isolation, Characterization, and Validation. *Appl Biochem Biotechnol* **2022**, 1-24, https://doi.org/10.1007/s12010-022-04221-y.
21. Sangilimuthu, A.Y.; Sivaraman, T.; Chandrasekaran, R.; Sundaram, K.M.; Ekambaram, G. Screening chemical inhibitors for alpha-amylase from leaves extracts of Murrayakoenigii (Linn.) and Aegle marmelos L. *J Complement Integr Med* **2021**, *18*, 51-57, https://doi.org/10.1515/jcim-2019-0345.
22. Patle, T.K.; Shrivas, K.; Kurrey, R.; Upadhyay, S.; Jangde, R.; Chauhan, R. Phytochemical screening and determination of phenolics and flavonoids in *Dillenia pentagyna* using UV–vis and FTIR spectroscopy. *Spectrochim. Acta A Mol. Biomol Spectrosc*. **2020**, *242*, 118717, https://doi.org/10.1016/j.saa.2020.118717.
23. Chethankumara, G.P.; Nagaraj, K.; Krishna, V.; Krishnaswamy, G. Isolation, characterization and *In vitro* cytotoxicity studies of bioactive compounds from Alseodaphne semecarpifolia Nees. *Heliyon* **2021**, e07325, https://doi.org/10.1016/j.heliyon.2021.e07325.
24. Hasballah, K.; Sarong, M.; Rusly, R.; Fitria, H.; Maida, D.R.; Iqhrammullah, M. Antiproliferative Activity of Triterpenoid and Steroid Compounds from Ethyl Acetate Extract of Calotropis gigantea Root Bark against P388 Murine Leukemia Cell Lines. *Sci. Pharm*. **2021**, *89*, 21, https://doi.org/10.3390/scipharm89020021.
25. Yadav, S.A.; Ramalingam, S.; Jebamalairaj, A.; Subban, R.; Sundaram, K.M. Biochemical fingerprint and pharmacological applications of *Barleria noctiflora* Lf leaves. *J. Complement. Integr. Med.* **2016**, *13*, 365-376, https://doi.org/10.1515/jcim-2015-0106.
26. Pandey, D.; Gupta, A.K. Bioactive Compound in *Urginea indica* (Kunth.) from Bastar and its Spectral Analysis by HPLC, UV-Vis, FT-IR, NMR, and ESI-MS. *SN Compr. Clin. Med*. **2019**, *1*, 241-254, https://doi.org/10.1007/s42399-018-0039-y.
27. Singh, R.; Bhardwaj, V.K.; Das, P.; Purohit, R. A computational approach for rational discovery of inhibitors for non-structural protein 1 of SARS-CoV-2. *Comput Biol Med* **2021**, *135*, 104555, https://doi.org/10.1016/j.compbiomed.2021.104555.
28. Si-Yuan, J.I.N.G.; Zi-Dan, W.U.; Zhang, T.H.; Zhang, J.; Zheng-Yi, W.E.I. *In vitro* antitumor effect of cucurbitacin E on human lung cancer cell line and its molecular mechanism. *Chin J Nat Med* **2020**, *18*, 483-490, https://doi.org/10.1016/S1875-5364(20)30058-3.
29. Verkhivker, G.M. Leveraging structural diversity and allosteric regulatory mechanisms of protein kinases in the discovery of small molecule inhibitors. *Curr Med Chem* **2017,** *4*, 4838-4872, https://doi.org/10.2174/0929867323666161006113418.
30. Rai, H.; Barik, A.; Singh, Y.P.; Suresh, A.; Singh, L.; Singh, G.; Nayak, U.Y.; Dubey, V.K.; Modi, G. Molecular docking, binding mode analysis, molecular dynamics, and prediction of ADMET/toxicity properties of selective potential antiviral agents against SARS-CoV-2 main protease: an effort toward drug repurposing to combat COVID-19. *Mol Divers* **2021**, *25*, 1905-1927, https://doi.org/10.1007/s11030-021-10188-5.
31. Parthasarathy, S.; Azizi, J.B.; Ramanathan, S.; Ismail, S.; Sasidharan, S.; Said, M.I.; Mansor, S.M. Evaluation of antioxidant and antibacterial activities of aqueous, methanolic and alkaloid extracts from *Mitragyna speciosa* (Rubiaceae family) leaves. *Mol*. **2009**, *14*, 3964-3974, https://doi.org/10.3390/molecules14103964.
32. Yadav, S.; Raj. A.; Sathishkumar, R. *In vitro* antioxidant activity of *Barleria noctiflora* L. f. *Asian Pac J Trop Biomed* **2012**, *2*, S716-S722, https://doi.org/10.1016/S2221-1691(12)60302-5.
33. GhasemiPirbalouti, A.; Siahpoosh, A.; Setayesh, M.; Craker, L. Antioxidant activity, total phenolic and flavonoid contents of some medicinal and aromatic plants used as herbal teas and condiments in Iran. *J Med Food* **2014**, *17*, 1151-1157, https://doi.org/10.1089/jmf.2013.0057.
34. Alu'datt, M.H.; Rababah, T.; Alhamad, M.N.; Al-Ghzawi, A.L.A.; Ereifej, K.; Gammoh, S.; Almajwal, A.; Hussein, N.M.; Raweshadeh, M. Optimization, characterization and biological properties of phenolic

compounds extracted from *Rosmarinus officinalis*. *J Essent Oil Res* **2017**, *29*, 375-384, https://doi.org/10.1080/10412905.2017.1331868.
35. Koottasseri, A.; Babu, A.; Augustin, A.; Job, J.T.; Narayanankutty, A. Antioxidant, Anti-Inflammatory and Anticancer Activities of the Methanolic Extract of *Thotteasiliquosa*: An *In vitro* and In Silico Study. Recent Pat Anticancer Drug Discov **2021**, *16*, 436-444, https://doi.org/10.2174/1574892816666210401143750.
36. Sufian, M.A.; Haque, M.R. Cytotoxic, thrombolytic, membrane stabilizing and antioxidant activities of *Hygrophilaschulli*. *Bangladesh J. Pharmacol*. **2015**, *10*, 692-696, https://doi.org/10.3329/bjp.v10i3.23718.
37. Anand, T.; Gokulakrishnan, K. Phytochemical analysis of *Hybanthus enneaspermus* using UV, FTIR and GC-MS. *IOSR J. Pharm*. **2012**, *2*, 520-524, http://dx.doi.org/10.9790/3013-0230520524.
38. AbdGhafar, S.Z.; Mediani, A.; Maulidiani, M.; Rudiyanto, R.; Ghazali, H.M.; Ramli, N.S.; Abas, F. Complementary NMR-and MS-based metabolomics approaches reveal the correlations of phytochemicals and biological activities in *Phyllanthus acidus* leaf extracts. *Food Res. Int*. **2020**, *136*, 109312, https://doi.org/10.1016/j.foodres.2020.109312.
39. Tong, Q.Y.; He. Y.; Zhao, Q.B.; Qing, Y.; Huang, W.; Wu, X.H. Cytotoxicity and apoptosis-inducing effect of steroidal saponins from *Dioscorea zingiberensis* Wright against cancer cells. *Steroids* **2012**, *77*, 1219-1227. https://doi.org/10.1016/j.steroids.2012.04.019.
40. Islam, M.S.; Parvin. M.S.; Islam, M.E. The protective and antioxidant effects of *Hygrophila schulli* seeds on oxidative damage of DNA and RBC cellular membrane. *Heliyon* **2022**, *8*, e08767, https://doi.org/10.1016/j.heliyon.2022.e08767.
41. Satpathy, S.; Patra, A.; Ahirwar, B.; Hussain, M.D. Process optimization for green synthesis of gold nanoparticles mediated by extract of *Hygrophila spinosa* T. Anders and their biological applications. *Phys E: Low-Dimens Syst Nanostructures* **2020**, *121*, 113830, https://doi.org/10.1016/j.physe.2019.113830.
42. Alshatwi, A.A.; Athinarayanan, J.; VaiyapuriSubbarayan, P. Green synthesis of platinum nanoparticles that induce cell death and G2/M-phase cell cycle arrest in human cervical cancer cells. *J Mater Sci Mater Med* **2015**, *26*, 1-9. https://doi.org/10.1007/s10856-014-5330-1.
43. Elengoe, A.; Sebestian, E. In silico molecular modelling and docking of allicin, epigallocatechin-3-gallate and gingerol against colon cancer cell proteins. *Asia-Pac J Mol Biol Biotechnol* **2020**, 51-67. https://doi.org/10.35118/apjmbb.2020.028.4.05.

Supplementary materials

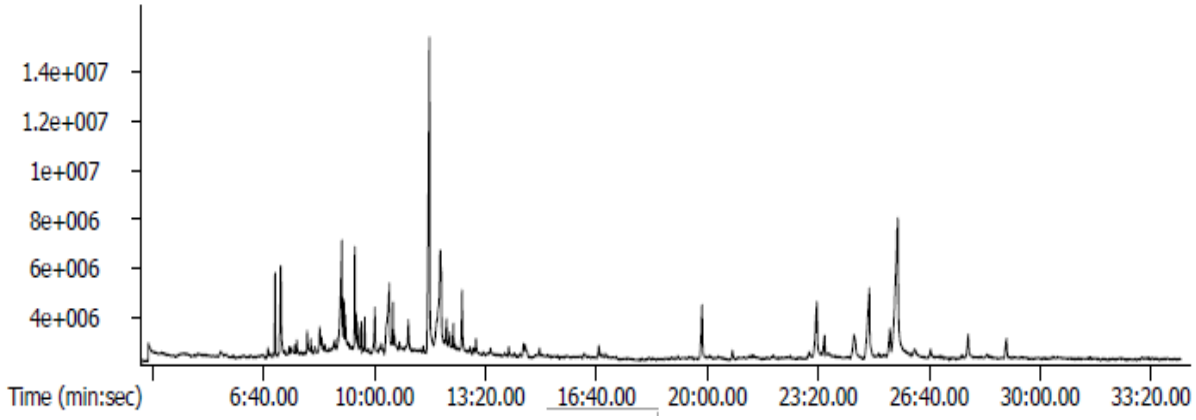

Figure S1. GC-MS chromatogram of chloroform extract of *H.schulli.*

Table S1. List of phytoconstituents identified in chloroform extract of *H.schulli* based on NIST library.

Peak	IUPAC Name, Chemical Formula and Molecular weight	Retention time	% Peak Area
1.	Ethyl Chloride; C_6H_7ClS; 146.63	03:13.2	10.74
2.	2,4-Decadienal; $C_{10}H_{16}O$; 152.23	05:10.1	0.02
3.	5,9-Undecadien-2-one, 6,10-dimethyl-, (E)-; $C_{20}H_{28}O_2S$; 332.50	06:30.0	0.22
4.	1,3-Butanediol, (R)-; $C_4H_9ClO_2$; 124.56	06:32.7	0.12
5.	2-Butanamine, (S)-; $C_{13}H_{19}NO$; 205.29	06:37.2	1.09
6.	Heptadecane,2,6,10,14-tetramethyl-; $C_{21}H_{44}$; 296.57	06:52.8	0.82
7.	Z-10-Pentadecen-1-ol; $C_{15}H_{30}O$; 226.39	06:57.9	0.56
8.	cis-13-Eicosenoic acid; $C_{20}H_{38}O_2$; 310.51	06:58.5	0.17
9.	Phenol, 2,4-bis(1,1-dimethylethyl)-; $C_{20}H_{26}O_2$; 298.41	07:00.2	16.29
10.	Heptadecane, 2,3-dimethyl-; $C_{20}H_{38}O_2$; 310.51	07:10.5	35.45
11.	2(4H)-Benzofuranone, 5,6,7,7a-tetrahydro-4,4,7a-trimethyl-; $C_{11}H_{16}O_2$; 180.24	07:12.9	3.94
12.	n-Decanoic acid; $C_{20}H_{40}O_2$; 312.53	07:25.8	1.80
13.	Dodecanoic acid; $C_{12}H_{24}O_2$; 200.31	07:26.2	1.80
14.	Diethyl Phthalate; $C_{12}H_{14}O_4$; 222.23	07:37.7	0.16
15.	Pentadecane, 2,6,10-trimethyl-; $C_{18}H_{38}$; 254.49	07:39.8	3.36
16.	13-Oxadispiro[5.0.5.1]tridecan-1-one; $C_{12}H_{18}O_2$; 194.27	07:40.6	0.77
17.	1-Naphthalenemethanol, 1,4,4a,5,6,7,8,8a-octahydro-2,5,5,8a-tetramethyl-; $C_{15}H_{26}O$; 222.36	07:58.2	6.86
18.	Methane, di-p-tolyl-; $C_{15}H_{14}Cl_2$; 265.17	08:02.5	0.10
19.	Ethanol, 2-(2-propenyloxy)-; $C_{13}H_{23}ClO_4$; 278.77	08:11.7	1.15
20.	5-Trimethylsilylpent-2-en-4-yne; $C_{16}H_{22}O_3Si$; 290.43	08:20.9	8.86
21.	3-Hydroxy-7,8-dihydro-á-ionol; $C_{13}H_{22}O_2$; 210.31	08:22.4	2.16
22.	Pentadecane, 2,6,10-trimethyl-; $C_{18}H_{38}$; 254.49	08:24.5	1.56
23.	Dodecane, 2,6,11-trimethyl-; $C_{15}H_{32}$; 212.41	08:27.2	0.82
24.	Propanoic acid, 2,2-dimethyl-, 2-(1,1-dimethylethyl) phenyl ester; $C_{15}H_{22}O_2$; 234.33	08:29.1	0.14
25.	1,1-Dodecanediol, diacetate; $C_{16}H_{30}O_4$; 286.40	08:30.5	0.69